Wave-to-Wire Model and Energy Storage Analysis of an Ocean Wave Energy Hyperbaric Converter

Paula B. Garcia-Rosa, *Student Member, IEEE*, José Paulo Vilela Soares Cunha, *Member, IEEE*, Fernando Lizarralde, *Member, IEEE*, Segen F. Estefen, Isaac R. Machado, and Edson H. Watanabe, *Senior Member, IEEE*

***Abstract*—This paper addresses the dynamic modeling and the energy storage analysis of a wave energy hyperbaric converter, which consists of a set of oscillating bodies (named as pumping modules) linked to hydropneumatic accumulators and an electric generating unit. A mathematical model of the accumulator is presented and a model for the generating unit is proposed, including a nonlinear model of a Pelton turbine. Then, the hydrodynamic, mechanical, and electrical characteristics of the subsystems that compose the converter are discussed. With the proposed model, it is possible to evaluate the dynamic behavior of the entire system. That is, for a given incident ocean wave, it is possible to evaluate all the system state variables and the generated electric power, including the quality (fluctuation, for example) of the generated voltage and frequency for islanded or power-grid-connected operation. Simulation results considering the proposed wave-to-wire model under the action of regular and irregular incident waves are presented to illustrate the performance of the system.**

***Index Terms*—Energy conversion, gas accumulator, ocean wave energy, Pelton turbine, wave to wire.**

NOMENCLATURE

A_a	Accumulator area.
A_o	Pipe area of the conduit.
A_p	Pump area.
A_w	Waterplane area.
c_p, c_v	Specific heat in constant pressure, and in constant volume processes.
e	Voltage.
e_a, e_b, e_c	Instantaneous stator voltages in phases a, b, c.
e_{th}	Grid voltage.
f	Electric frequency.
f_e	Wave excitation force.
f_p	Power takeoff force.
g	Acceleration due to gravity.
H_s	Significant wave height.
H_w	Wave height.
i	Electric current.
i_a, i_b, i_c	Instantaneous stator currents in phases a, b, c.
J_m	Moment of inertia of the generator and turbine.
k_N	Proportional constant of the needle.
l_o	Conduit length.
L_l, L_m	Leakage inductance, magnetizing inductance.
m, m_h	Mass and added mass of the floating body.
m_g	Mass of gas.
N	Total number of floating bodies.
n_f	Number of field poles.
p	Pressure in the turbine conduit.
p_c	Chamber pressure.
p_p	Pump pressure.
P_e, P_m	Electrical power, mechanical power.
Q_i, Q_o	Input flow, output flow.
$Q_{i,\text{avg}}$	Average value of the input flow.
R	Electrical resistance.
R_h	Radiation damping coefficient.
$\mathcal{R}_g$	Universal gas constant.
t	Time.
T_e, T_m	Electrical torque, mechanical torque.
t_p	Peak period of the wave.
t_w	Period of the wave.

Manuscript received June 28, 2011; revised February 10, 2012, August 03, 2012, and February 12, 2013; accepted April 25, 2013. Date of publication July 25, 2013; date of current version April 10, 2014. This work was supported in part by the Brazilian agencies CAPES, CNPq, and FAPERJ, and Tractebel Energia (ANEEL R&D Program).

Guest Editor: Y. Li.

P. B. Garcia-Rosa and S. F. Estefen are with the Department of Ocean Engineering, Instituto Alberto Luiz Coimbra de Pós-Graduação e Pesquisa em Engenharia (COPPE), Universidade Federal do Rio de Janeiro, Rio de Janeiro 21945-970, Brazil (e-mail: paula.bgr@gmail.com).

J. P. V. S. Cunha is with the Department of Electronics and Telecommunication Engineering, Universidade do Estado do Rio de Janeiro, Rio de Janeiro 20550-013, Brazil.

F. Lizarralde and E. H. Watanabe are with the Department of Electrical Engineering, Instituto Alberto Luiz Coimbra de Pós-Graduação e Pesquisa em Engenharia (COPPE), Universidade Federal do Rio de Janeiro, Rio de Janeiro 21945-970, Brazil.

I. R. Machado is with the Department of Electrical Engineering, Universidade Federal do Ceará, Sobral 62010-560, Brazil.

Color versions of one or more of the figures in this paper are available online at http://ieeexplore.ieee.org.

Digital Object Identifier 10.1109/JOE.2013.2260916

$\mathcal{T}_g$	Gas absolute temperature.
v	Velocity of the floating body.
V_a	Water volume in the accumulator.
V_c	Volume of the hyperbaric chamber.
V_g	Volume of gas.
v_o	Water velocity in the conduit.
V_T	Total volume of water and gas.
x_a	Piston position of the accumulator.
x_N	Needle position.
Z_L	Load impedance.
Z_{th}	Grid impedance.
γ	Specific heat ratio of the gas.
ζ	Water surface elevation.
θ	Angle between d-axis and magnetic axis of phase a in electrical radians.
η_m	Hydraulic turbine efficiency.
ρ, ρ_w	Freshwater density, seawater density.
ϕ	Magnetic flux.
ω	Wave frequency.
ω_m, ω_r	Angular speed of the rotor in mechanical radians per second, in electrical radians per second.

Subscripts

n	Index of a floating body.
d, q	Reference frames.
r, s	Rotor, stator.
f	Field.

I. Introduction

OCEAN wave energy is a renewable and nonpolluting resource with a worldwide potential estimated at the order of 2000 TWh/year [1] that can contribute significantly to the demand for electricity. Although it has not yet been commercially exploited, research and development on wave energy technologies have been conducted for more than three decades.

Several wave energy converters (WECs) with different processes of energy conversion are available from laboratory experiments and prototype tests. Recent reviews indicate that there are about 100 projects at various stages of development [2]. According to the working principle, WECs can be classified as oscillating water column (OWC) systems, overtopping devices, or oscillating-body systems. In the oscillating-body systems, a floating body may be connected to a hydraulic system before the electrical energy conversion, e.g., [3]–[5], or may be connected to a direct-drive electric generator, e.g., [6]–[9].

The wave power varies in several time scales: from wave to wave (seconds), according to the sea state (hours), and according to seasonal variations (months). Thus, regardless of the energy conversion process, without any method of energy storage, the variation of the power output from a WEC can be quite large, as may occur in other intermittent renewable sources, such as wind or solar energy. Energy storage allows the smoothing of the output power that is generated from a highly variable input power [3], as in the conversion system analyzed here.

Some examples of energy storage technologies that have been investigated and implemented in renewable energy systems are: compressed-air energy storage, hydrogen-storage systems, flywheels, batteries, supercapacitors, and superconducting magnetic energy storage [10].

In wave energy technologies, there are basically three methods used as a short-term energy storage (range of ten seconds to a minute)[4]: potential energy storage in water reservoirs is applied to some overtopping systems [11], and kinetic energy (flywheel) in OWC systems with air turbines and gas accumulators are applied to some oscillating-body systems [3].

The design of a wave energy conversion system is usually based on numerical simulations and tests with small-scale models at ocean basin laboratories. The obtained results with these methods are fundamental to improve and optimize the design of selected configurations. Different versions of a WEC may be evaluated with numerical models at relatively low costs and, then, a small-scale model is usually tested to validate the numerical results and to investigate phenomena which are not evidenced by simulations [12]. The different numerical methods usually used for modeling WECs are systematically reviewed in [13].

Moreover, the numerical models are useful to evaluate and estimate the generated power according to typical sea states of an installation site and to verify the performance and feasibility of control strategies, which are included to improve global performance and reliability of the system. These strategies may be designed to improve the absorption of wave energy, e.g., [4] and [14], and to deal with emergency procedures (interlocking mechanisms) and the quality of the electricity supplied by the WEC.

Designing efficient WECs and their control systems depends on mathematical models of hydrodynamic, mechanical, and electrical characteristics of their subsystems. The hydrodynamic model of oscillating body systems is described in some standard wave energy literature, such as the book by Falnes [15]. Some recently published works, e.g., [5], [16], and [17], describe the dynamic model of different WECs from the incident wave to the electrical power delivered to the grid, also known as the wave-to-wire model. In [18], a generic model of a system with hydraulic power takeoff is developed. A wave-to-wire model allows prior knowledge of the dynamic behavior of the plant considering interaction between each subsystem, which enables the identification of dynamical effects that are not evidenced if the models are considered separately.

This paper addresses the wave-to-wire model and the energy storage analysis of the Brazilian wave energy hyperbaric converter [19]. This energy converter consists of a set of oscillating bodies (named as pumping modules), a two-stage accumulator linked to a hyperbaric chamber, which was previously pressurized, and an electric generating unit. The water flow obtained from the body motion is displaced to the accumulator, and then,

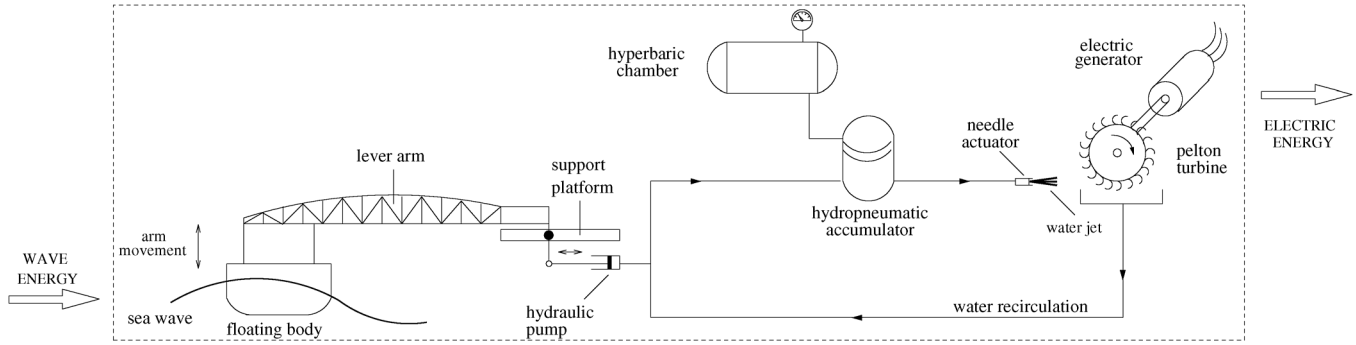

Fig. 1. Schematic of the wave energy converter.

a pressurized water flow operates a Pelton turbine coupled to an electrical generator. Such arrangement is different from other oscillating-body systems which include hydraulic power takeoff (PTO) mechanisms with high-pressure and low-pressure gas accumulators. In these systems, a machine (motor or turbine) is driven by the flow resulting from the pressure difference between accumulators [4]. Additionally, the applied pressure in the hyperbaric converter is in the range 250–500 m of water column, which is substantially higher than some proposed concepts.

In previous works related to hyperbaric converters, e.g., [20]–[23], the dynamic models of the pumping unit and the generating unit were developed apart. The complete system dynamics, including both units, has never been considered. The model of a pumping module is presented in [20] with numerical simulations and experimental results (in small scale 1 : 10). Based on this model, the problem of optimizing the efficiency of the primary conversion is discussed in [21] together with a latching control strategy, and, in [22], a strategy based on phase control concepts is also proposed to improve the absorption of wave energy. In this case, a sliding mass attached to the arm is used to modify the dynamics of the floating body. A simplified linear model of the generating unit, which assumes constant pressure in the accumulator, is described in [23], where a hydraulic turbine speed controller is proposed to regulate the speed of the turbine at a rated value. The control strategy is based on cascade control combined with feedforward of electric load disturbances.

From the models developed so far, the connection between the pumping unit dynamics and the electrical unit dynamics is not possible, since the model of the turbine is simplified and both units do not account for oscillations in the pressure of the system. Besides, the development of the accumulator model is fundamental to integrate these units.

In this work, we develop the dynamic model of the accumulator, and then, a dynamic equation for the pressure of the system is presented. A mathematical model of the generating unit is proposed, where the nonlinear model of the hydraulic turbine depends on the pressurized water flow and the pressure, and the electric generator dynamics complements the wave-to-wire model. Then, from the wave input power, we can evaluate the electrical output power and the generated frequency and generated voltage by the WEC. The hydrodynamic, mechanical, and electrical characteristics of the main subsystems are discussed.

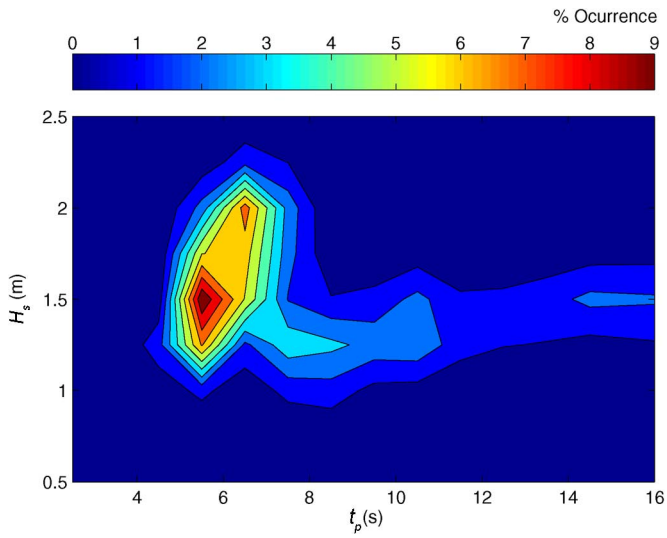

Fig. 2. Sea-state occurrence at Port of Pecém, Brazil.

The dynamics of the entire process and its energy storage are evaluated. Simulation results considering the proposed wave-to-wire model under the action of regular and irregular incident waves illustrate the performance of the WEC, when it is connected to an islanded system or to the power grid.

II. Wave Energy Hyperbaric Converter

The hyperbaric converter is composed of pumping modules, a hydropneumatic accumulator, a hyperbaric chamber, and a generating unit [22], as illustrated in Fig. 1.

In this system, each pumping module has a floating body linked to a hydraulic pump through a lever arm. The vertical motion of the body due to the wave action induces the pump actuator to displace water obtained from a closed circuit to the accumulator, which has an internal piston separating water from gas. Then, the pressurized water flow from the accumulator operates a Pelton turbine coupled to an electrical generator. The water flow can be controlled through a needle actuator.

A full-scale prototype of this WEC with two pumping modules and a 125-kVA synchronous generator is currently being installed at Port of Pecém, Ceará State, Brazil. In what follows, an overview of the wave climate in the installation site is described and a block diagram of the wave-to-wire model is depicted.

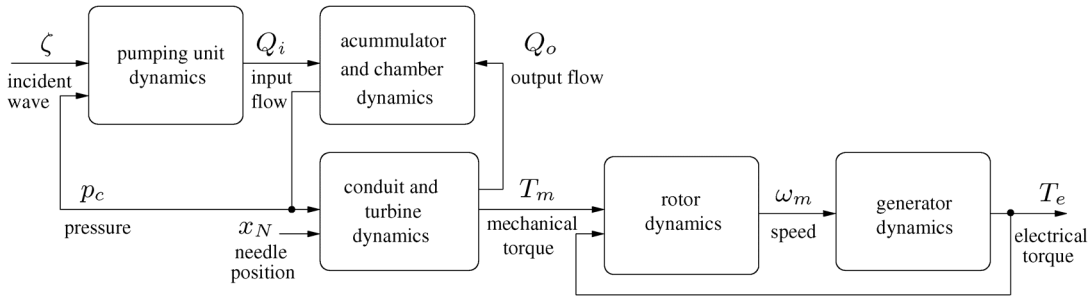

Fig. 3. Basic block diagram of the wave-to-wire model.

A. Overview of the Wave Climate in the Brazilian Northern Coast

Considering its northwest–southeast (NW–SE) coastline orientation, the Brazilian northern coast is exposed to wave fields generated in both hemispheres, and a similar mode of variability is observed in the wave climate. In the winter season, locally generated southeastern waves are predominant, while northern swells prevail over local sea conditions during summer [24].

Fig. 2 illustrates the scatter diagram representing the occurrence of sea states at the coast of Port of Pecém. Wave data were obtained through some *in situ* measurements using a Datawell Directional Waverider buoy during a five-year program led by the National Institute of Waterways Research (INPH), and then, an analysis of the wave climate was done in [24].

Initial analysis has shown a predominance of small waves, between 1 and 1.75 m of significant wave height (H_s), despite some recordings of waves higher than 2 m. Peak wave period (t_p) values are predominantly short, in the range of 5–7 s, but the occurrence of waves with long periods (12–20 s) coming from the north hemisphere has also been recorded. The occurrence of these swells coincides with the cold seasons (and some associated storms) in the north Atlantic [19].

B. Description of the Wave-to-Wire Model

A block diagram of the wave-to-wire model describing the hyperbaric converter is presented in Fig. 3. It can be noted that the pressure oscillations may affect both pumping module and generating unit dynamics. Since the accumulator connects these subsystems, its dynamic model is needed for the evaluation of the oscillations in the system variables (e.g., pressure, flow, turbine speed, and electric-generated power), which are induced by the oscillatory behavior of the waves.

In [23], a simplified linear model representing the small-signal performance of the turbine is considered in the design of a turbine speed governor. Such a model does not consider large variations in the input power due to the intermittent characteristic of the waves. In this work, a nonlinear model is described, which is more appropriate for large-signal performance analysis of the turbine. In this case, the dynamics of the accumulator and the oscillations both in pressure and output flow are also taken into account.

III. Pumping Modules Model

The pumping modules dynamics are described by the motion of the floating bodies. Here, we assume only heave oscillatory motion and neglect wave interaction effects between bodies. Consider the case of a system with N identical pumping modules. Then, the motion of the nth body is given by the following governing equation [15]:

$$m\dot{v}_n(t) = f_{h,n}(t) + f_{s,n}(t) + f_{p,n}(t) \tag{1}$$

where the body oscillates under the action of hydrodynamic forces (f_h), hydrostatic force (f_s), and the vertical force due to the PTO mechanism (f_p). Since linear hydrodynamic theory [15] is considered, the hydrodynamic forces are given by the superposition of the excitation force (f_e), which is the force on the body held fixed in incident waves, and the radiation force (f_r), which is the force due to the body oscillation in the absence of waves.

Thus, the vertical motion of the body satisfies the integro-differential equation

$$[m + m_h(\infty)]\,\dot{v}_n(t) + \int_0^t K(t-\tau)v_n(\tau)d\tau + g\rho_w A_w \int_0^t v_n(\tau)d\tau = f_{e,n}(t) + f_{p,n}(t) \tag{2}$$

where the kernel of a convolution term is known as the fluid memory term and is given by [25]

$$K(t-\tau) = \frac{2}{\pi}\int_0^\infty R_h(\omega)\cos\left[\omega(t-\tau)\right]d\omega. \tag{3}$$

In this case, the PTO force is applied by the pump to the body, which is given by

$$f_{p,n}(t) = A_p p_{p,n}(t), \quad p_{p,n}(t) \approx \begin{cases} 0, & v_n(t) \geq 0 \\ p_c, & v_n(t) < 0. \end{cases} \tag{4}$$

Equation (4) indicates that the body motion injects water into the accumulator exclusively during the descending motion of the body, when the pressure inside the pump p_p becomes equal to the chamber pressure p_c (high-pressure stage). During the ascendant motion of the body, the pressure inside the pump becomes negligible (low-pressure stage) [20].

For regular waves of frequency ω and height H_w, the wave excitation force is given by [15]

$$f_e(t) = F_e(\omega)\cos\omega t, \quad F_e(\omega) = H_w\sqrt{\frac{\rho g^3 R_h(\omega)}{2\omega^3}} \tag{5}$$

when considering axisymmetric bodies. For irregular waves

$$f_e(t) = \sum_{i=1}^{N_i} f_{e,i}(t) \tag{6}$$

which is a linear combination of N_i regular waves. This is a numerical approximation of real waves that are characterized by defining a spectrum with a significant wave height H_s, a peak wave period t_p, and by using a random phase generator [15].

Finally, the water flow input into the accumulator $Q_{i,n}(t)$ can be calculated by

$$Q_{i,n}(t) = \begin{cases} 0, & v_n(t) \geq 0 \\ A_p v_n(t), & v_n(t) < 0 \end{cases} \tag{7}$$

where the velocity v_n is the solution of (2). Then, the total input flow is

$$Q_i(t) = \sum_{n=1}^{N} Q_{i,n}(t). \tag{8}$$

The power of the incident wave train is expressed in kilowatts per meter of wavefront as

$$P_w = k_w H_w^2 t_w \tag{9}$$

where H_w and t_w are, respectively, the height and the period of the incident wave and $k_w = (\rho g^2/32\pi) \times 10^{-3}$ kg/m/s^4, for the sinusoidal regime or $k_w \approx 0.49$ kg/m/s^4 for the irregular regime [15]. Note that, for irregular waves, $H_w = H_s$ is the significant wave height and $t_w = t_p$ is the peak wave period.

The mean power extracted by each floating body during a time interval T is given by

$$P_{a,n} = \frac{1}{T} \int_0^T f_{p,n}(t) v_n(t) dt. \tag{10}$$

A correlation between numerical simulations and experimental results of the absorbed power per floating body (in kilowatts) was carried out in [20] to validate the pumping unit model. The experimental results were obtained with a small-scale model (1 : 10) with four pumping modules, tested in the ocean basin at LabOceano, COPPE, Federal University of Rio de Janeiro (Rio de Janeiro, Brazil), as illustrated in Fig. 4. The model was submitted to different regular waves, with heights and periods representative of the Brazilian south coast.

IV. Accumulator Model

The internal section of the hydropneumatic accumulator is divided into air and water separated by a piston, as illustrated in Fig. 5. Thus, when the inflow of water Q_i is greater than the output flow Q_o (water released to the hydraulic turbine), the piston rises up, storing the captured energy in the form of compressed air. Conversely, when the output flow is greater than the inflow, the piston moves down, releasing the previously stored energy. Based on this fact, the volume of water inside the accumulator $V_a(t)$ is governed by the law of conservation of mass

$$\dot{V}_a(t) = Q_i(t) - Q_o(t) \tag{11}$$

Fig. 4. Small-scale pumping modules at LabOceano.

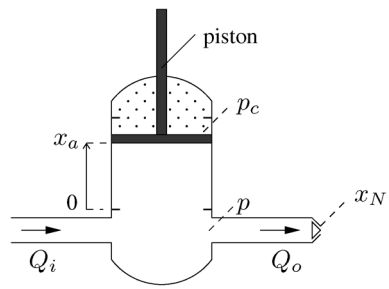

Fig. 5. Schematic representation of the hydropneumatic accumulator.

and the position of the internal piston $x_a(t)$ satisfies

$$\dot{x}_a(t) = \frac{1}{A_a} \left[Q_i(t) - Q_o(t) \right]. \tag{12}$$

Following the approach of [4], we assume that the gas compression/expansion process inside the accumulator is an isentropic process (negligible heat transfer) and the gas temperature is approximately constant and equal to the environmental temperature during a sea state. Then, the pressure p_c (from Fig. 5) is obtained by the equation of an ideal gas

$$p_c(t) V_g^{\gamma}(t) = m_g \mathcal{R}_g \mathcal{T}_g \tag{13}$$

where $\gamma = c_p/c_v$ is the specific-heat ratio for the gas. The volume of gas (V_g) can be calculated by the difference between the total volume of water and gas (V_T) and the volume of water in the accumulator

$$V_g(t) = V_T - V_a(t). \tag{14}$$

After differentiation of (13) and (14) with respect to time, the following nonlinear differential equation for the chamber pressure can be obtained:

$$\dot{p}_c = \gamma m_g \mathcal{R}_g \mathcal{T}_g \frac{(Q_i - Q_o)}{(V_T - V_a)^{\gamma+1}}. \tag{15}$$

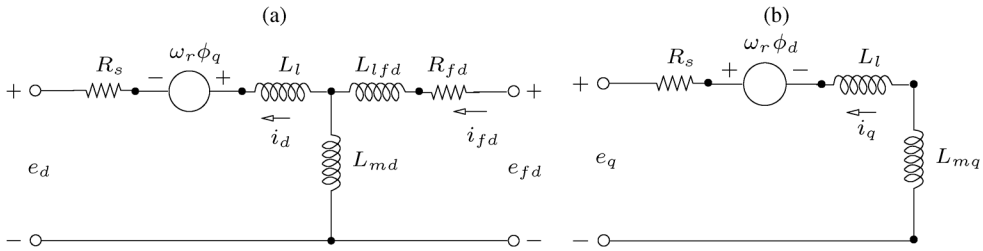

Fig. 6. Equivalent electric circuit of the synchronous generator: (a) d-axis and (b) q-axis.

V. Generating Unit Model

This section presents the nonlinear model of the hydraulic turbine, which includes the water dynamics in the conduit and the model of the electric generator.

A. Hydraulic Turbine Dynamics

The turbine and conduit characteristics are determined by equations relating the acceleration of water column and the velocity of water in the conduit and the turbine mechanical power [26]. Additionally, we consider the following assumptions:

- A1) the pressure losses in the conduit and needle are negligible;
- A2) the water pipe is inelastic and the water is incompressible;
- A3) the velocity of the water varies directly with the needle opening;
- A4) the mechanical power of the turbine is proportional to the product of pressure and water flow through the turbine.

From assumptions A1)–A3) and Bernoulli's equation, the pressure in the conduit is given by [27]

$$p(t) = \frac{\rho v_o^2(t)}{2k_N^2 x_N^2(t)}, \qquad x_N(t) > 0. \tag{16}$$

From assumption A2), the acceleration of water column in the conduit is characterized by Newton's second law of motion and can be expressed as

$$\rho l_o A_o \dot{v}_o = A_o(p_c - p). \tag{17}$$

The output flow from the accumulator Q_o is proportional to the velocity of the water in the conduit, that is, $Q_o(t) = A_o v_o(t)$. Thus, from (17), the water flow rate is given by

$$\dot{Q}_o = \frac{A_o}{\rho l_o}(p_c - p). \tag{18}$$

According to assumption A4) and considering η_m the hydraulic efficiency of the turbine, the mechanical output power is given by

$$P_m = \eta_m Q_o p. \tag{19}$$

From the mechanical power (19), it is possible to calculate the torque in the turbine shaft as

$$T_m = \frac{P_m}{\omega_m} \tag{20}$$

where ω_m is the angular speed, given by the torque balance in the turbine-generator shaft, as will be shown in (33).

B. Electric Generator Model

A three-phase synchronous machine is used as the electric generator in the hyperbaric converter. A detailed dynamic model of a synchronous machine is developed in [28]. Here, we adopt a simplified model which takes into account the dynamics of the stator and field windings circuit, assumes balanced loads, and neglects the damper windings. Fig. 6 shows the equivalent electric circuits represented in the rotor reference frame (dq frame).

The main advantage of using the dq frame is that the sinusoidal quantities reduce to direct current (dc) quantities, and then, simplified calculations can be performed before recovering it to real alternating current (ac) variables. The three-phase a, b, and c variables of the machine are turned into the dq reference frame variables by using the dq transformation, which is given by

$$\begin{bmatrix} e_d \\ e_q \end{bmatrix} = M_{dq} \begin{bmatrix} e_a \\ e_b \\ e_c \end{bmatrix} \tag{21}$$

with

$$M_{dq} = \frac{2}{3} \begin{bmatrix} \cos(\theta) & \cos\left(\theta - \frac{2\pi}{3}\right) & \cos\left(\theta + \frac{2\pi}{3}\right) \\ -\sin(\theta) & -\sin\left(\theta - \frac{2\pi}{3}\right) & -\sin\left(\theta + \frac{2\pi}{3}\right) \end{bmatrix} \tag{22}$$

where θ is the angle by which the d-axis leads the magnetic field axis of phase a winding in the direction of rotation

$$\dot{\theta} = \omega_r \tag{23}$$

and ω_r is the rotor angular speed in electrical radians per second, as is illustrated in Fig. 7 [27].

The currents in the dq frame can be expressed in terms of flux linkages as

$$i_d = -\frac{\phi_d - \phi_{md}}{L_l} \tag{24}$$

$$i_q = -\frac{\phi_q}{L_l + L_{mq}} \tag{25}$$

$$i_{fd} = -\frac{\phi_{md} - \phi_{fd}}{L_{lfd}} \tag{26}$$

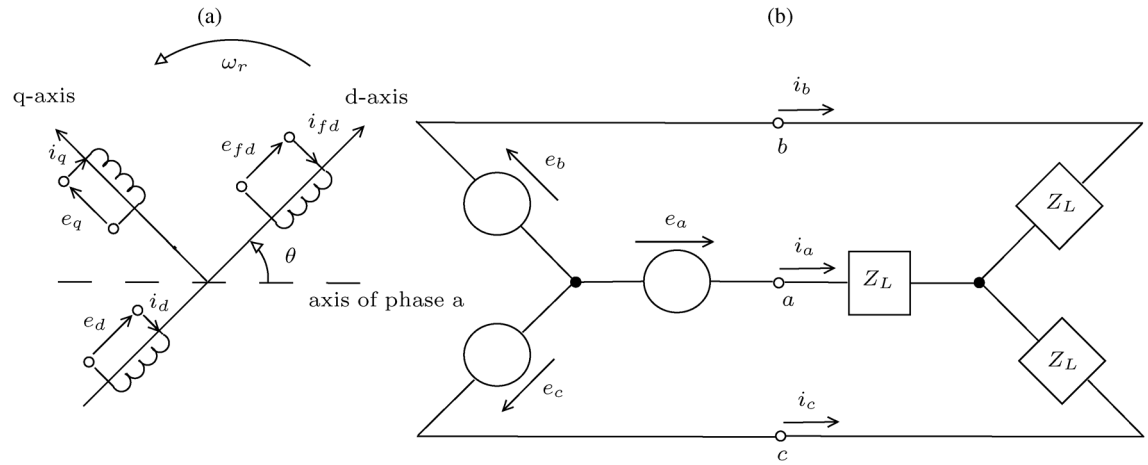

Fig. 7. Synchronous generator circuits: (a) rotor and stator in the dq frame and (b) stator connected to a three-phase load.

where the mutual flux linkage is $\phi_{md} = L_{md}(i_{fd} - i_d)$ and the other flux linkages obey the differential equations

$$\dot{\phi}_d = e_d + \phi_q \omega_r + R_s i_d \tag{27}$$

$$\dot{\phi}_q = e_q + \phi_d \omega_r + R_s i_q \tag{28}$$

$$\dot{\phi}_{fd} = e_{fd} - R_{fd} i_{fd}. \tag{29}$$

Finally, the instantaneous electrical power at the machine terminal is given by

$$P_e = \frac{3}{2}(e_d i_d + e_q i_q) \tag{30}$$

and the electromagnetic torque is

$$T_e = \frac{3 n_f}{4}(\phi_d i_q - \phi_q i_d). \tag{31}$$

Moreover, the relationship between speed ω_r in electrical units and the corresponding speed in mechanical units is given by

$$\omega_r = \frac{n_f}{2}\omega_m. \tag{32}$$

According to Newton's second law, the angular speed of the rotor (ω_m) in mechanical radians per second is governed by the following differential equation:

$$\dot{\omega}_m = \frac{1}{J_m}(T_m - T_e - T_{nl}) \tag{33}$$

where the nonload torque T_{nl} represents core losses due to hysteresis and eddy currents, and rotational losses due to friction and windage.

When there is an imbalance between the turbine and generator torques, the net torque causes rotor acceleration (or deceleration). Since the generator is a synchronous machine, the generated frequency f is proportional to the rotor speed

$$f = \frac{n_f}{4\pi}\omega_m \tag{34}$$

and the root mean square (rms) terminal voltage is given by

$$e = \sqrt{e_d^2 + e_q^2}. \tag{35}$$

The electric generator can be connected to the power grid or to an islanded system. In this framework, the quality of the electricity supplied must meet requirements with respect to limits of variations in the generated frequency and voltage, as well as the level of reliability [27]. For these purposes, voltage and frequency controllers can be applied in synchronous generators, or other schemes with additional power electronics may be adopted to maintain the generated frequency and voltage within acceptable limits, e.g., [17]. Here, the traditional techniques generally used in hydropower plants, without specific power electronics circuits, may be considered to obtain an acceptable power quality, provided that the energy storage employed by the hyperbaric converter gives a sufficiently smooth output. In this case, the frequency may be controlled by modifying the water flow to the Pelton turbine, and a conventional excitation control system may be adopted to regulate the voltage.

VI. Simulation Results

With the developed wave-to-wire model, it is possible to study the dynamic performance of this WEC. For this study, some steps need to be followed: 1) generate the incident wave train ζ; 2) define the generator field voltage e_{fd}; and 3) choose the type of operation: islanded or connected to the power grid. In the case of islanded operation, the three-phase currents are defined by the load impedance Z_L (Fig. 7). Besides, in the other case, the grid is represented by a Thévenin equivalent circuit, that is, a voltage source e_{th} in series with a given impedance Z_{th}. In both cases, the balanced operation is assumed.

The simulations of the hyperbaric converter dynamics were performed considering one axisymmetric floating body (Section VI-A) and two bodies (Section VI-B) with $m = 25 \times 10^3$ kg in the pumping unit. The added mass m_h and radiation resistance R_h coefficients were computed by the software WAMIT [29].

The accumulator area is $A_a = 0.57$ m^2 and other main parameters are: $V_T = 6.34$ m^3, $\mathcal{R}_g = 0.287$ kJ/kg/K, $\mathcal{T}_g = 300$ K, $\gamma = 1.4$, and $\eta_m = 0.85$. The initial values of gas volume and chamber pressure are, respectively, $V_g = 5.5$ m^3 and $p_c = 2.5$ MPa (255 m of water column). The main parameters of the synchronous generator (WEG GTA202CMVJ, Brazil) are given in

TABLE I
PARAMETERS OF THE SYNCHRONOUS GENERATOR

Parameter	Symbol	Value	Unit
Rated power	S_N	125	kVA
Rated voltage	e_N	380	V
Rated frequency	f_N	60	Hz
Field poles	n_f	4	–
Stator resistance	R_s	0.016	ohms
Power losses (no-load)	P_{nl}	2.6	kW

Table I and the grid parameters were chosen as $e_{th} = e_N$ and $Z_{th} = (e_{th}^2/3S_N)(0.1 - j0.0027)$.

An excitation system provides direct current to the field winding of the generator and performs regulation of its terminal voltage. Here, a system of the type DC1A [30] is adopted. The simulations are performed without frequency controllers, and then, for the islanded system, the load impedance Z_L is a pure three-phase balanced resistance calculated to consume an average power equal to the mechanical power, which comes from the waves. Furthermore, the needle position is chosen to balance the output flow from the accumulator to the average of the input flow from the pumps.

A. Energy Storage Analysis

The first simulation results allow the analysis of the energy storage of the hyperbaric converter. Since the wave power has an oscillatory nature, the instantaneous absorbed power by the floating bodies can suddenly fluctuate from zero to maximum values. The aim of such analysis is to numerically evaluate the smoothing characteristic of the system to obtain acceptable power quality on the output for fast oscillations of the incident wave (range of seconds). In general, an acceptable limit of electric frequency fluctuation is ±2% [31] and an acceptable limit of voltage fluctuation is ±5%.

The generator is connected to an islanded system, and the converter is submitted to incident regular waves of period $T_w = 6$ s and height $H_w = 1.4$ m, with a wave-power level of approximately 11.5 kW/m. In these simulations, the oscillations on the variables are calculated according to the following equation:

$$\Delta x = \left(\frac{x_{\max} - x_{\min}}{x_{\min}} \right) \times 100\% \tag{36}$$

where x is the variable, $x_{\max}$ is the maximum value observed, and $x_{\min}$ is the minimum value of x during a simulation. Tables II and III illustrate the obtained oscillations for the pressure, the output flow, the mechanical and electrical powers, the generated frequency, and the voltage, when the volume of the hyperbaric chamber V_c and the volume of the hydropneumatic accumulator V_a are, respectively, multiplied and divided by a factor equal to 10.

It can be observed that in both cases (changes in V_c and V_a), the values of the variables have larger oscillations as the volume of the equipment becomes smaller. However, the variables have the lowest oscillations for the highest value of the chamber volume $(10V_c)$, when compared to the highest volume of the accumulator $(10V_a)$. Indeed, the volume of the accumulator is divided into water and gas, and the chamber has the greatest volume of gas. The hyperbaric chamber is responsible for smoothing the oscillations. However, the discharge duration of the storage is enhanced by increasing the volume of the hydropneumatic accumulator. From (11) and considering constant output flow at a rated value, the full power duration of the storage is estimated at the order of 30 s.

TABLE II
FLUCTUATIONS FOR DIFFERENT VALUES OF THE HYPERBARIC CHAMBER VOLUME ($V_c = 4.65$ m^3)

	0.1 V_c	V_c	10 V_c
ΔQ_o%	3.321	0.796	0.090
Δp%	6.544	1.614	0.180
ΔP_m%	9.643	2.372	0.274
ΔP_e%	0.048	0.021	0.001
Δf%	3.001	0.739	0.081
Δe%	0.052	0.014	0.001

TABLE III
FLUCTUATIONS FOR DIFFERENT VALUES OF THE ACCUMULATOR VOLUME ($V_a = 1.69$ m^3)

	0.1 V_a	V_a	10 V_a
ΔQ_o%	0.802	0.796	0.793
Δp%	1.620	1.614	1.555
ΔP_m%	2.429	2.372	2.364
ΔP_e%	0.023	0.021	0.021
Δf%	0.750	0.739	0.738
Δe%	0.015	0.014	0.014

TABLE IV
ELECTRICAL POWER, FREQUENCY, AND VOLTAGE FLUCTUATIONS FOR DIFFERENT VALUES OF THE COMBINED MOMENT OF INERTIA ($J_m = 25.6$ kg m^2)

	J_m	5 J_m	10 J_m
ΔP_e%	0.021	0.002	0.001
Δf%	0.739	0.141	0.070
Δe%	0.014	0.001	0.001

The fluctuations in the electric frequency are around the oscillations of the output flow, and the oscillations of the electrical power are small when compared to the oscillations of the mechanical power. It can be observed that, for the smallest volume of the hyperbaric chamber $(0.1V_c)$, the frequency fluctuations exceed 2%.

A new trend for energy storage in renewable energy systems is to combine several storing technologies [10], e.g., in [32], Murray *et al.* integrate supercapacitors with the inertia of a Wells turbine. In the hyperbaric converter, a storage system that integrates gas accumulators and flywheel energy storage can be applied. Flywheels are commonly used due to the simplicity of storing kinetic energy in a spinning mass [10]. Table IV illustrates the obtained oscillations for the electrical power, frequency, and terminal voltage when a flywheel with different moments of inertia (combined with the moment of inertia of the generator and the turbine) is attached to the turbine shaft.

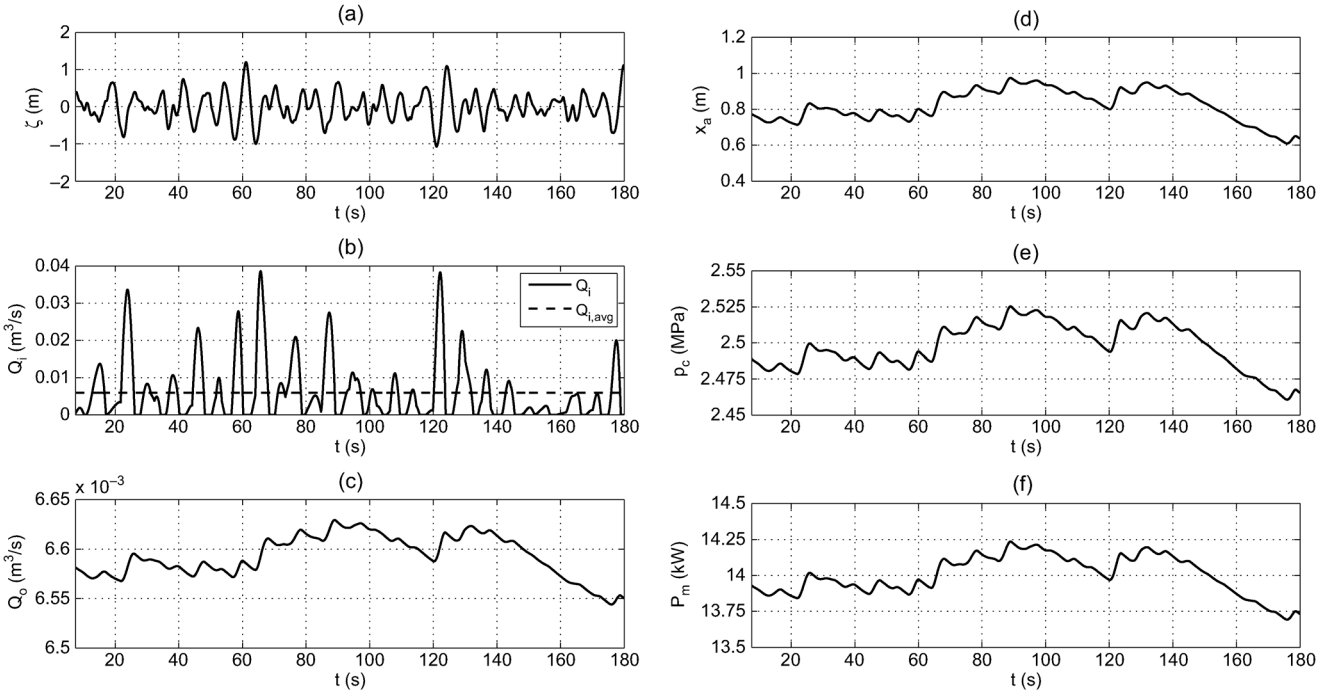

Fig. 8. Simulation results: Pumping unit variables and mechanical power for the islanded system and the connected system.

It can be noted that the electric frequency fluctuations are smaller for larger moments of inertia, as expected. The flywheel affects directly the fluctuations on generator speed and, consequently, the frequency fluctuations. Besides, the buffering capacity of the chamber affects directly the fluctuations on output flow, pressure, and mechanical power, and consequently, this affects the fluctuations on electrical power, frequency, and terminal voltage. This analysis can be used to verify the design of the energy storage system to obtain acceptable power oscillations without oversizing the main equipment. For an islanded system, a small chamber and a flywheel could be a solution for storage with reduced structural costs.

B. Islanded System and Grid Connection

A Pierson–Moskowitz spectrum [33] is used to generate an incident wave train with significant wave height $H_s = 1.4$ m, peak wave period $t_p = 6.2$ s, and random phase. This sea state is representative of the wave climate in Port of Pecém, illustrated in Fig. 2. The wave-power level is 5.96 kW/m. Two different methods are commonly used to simulate the time series of ocean waves, given a target power spectrum: the random phase scheme and the random coefficient scheme [34]. Here we consider the first one.

Figs. 8–10 show the simulation results, when the hyperbaric converter is an islanded system and when it is connected to the grid. Each simulation was performed for the same time series, thus the variables of the pumping unit and the mechanical power exhibit the same results (Fig. 8).

The output flow Q_o [Fig. 8(c)] is about the average value $(Q_{i,\mathrm{avg}})$ of the input flow Q_i [Fig. 8(b)], which shows the smoothing characteristic obtained by the hyperbaric chamber. From Fig. 8(d) and (e), the oscillations in the piston position and the chamber pressure can be observed.

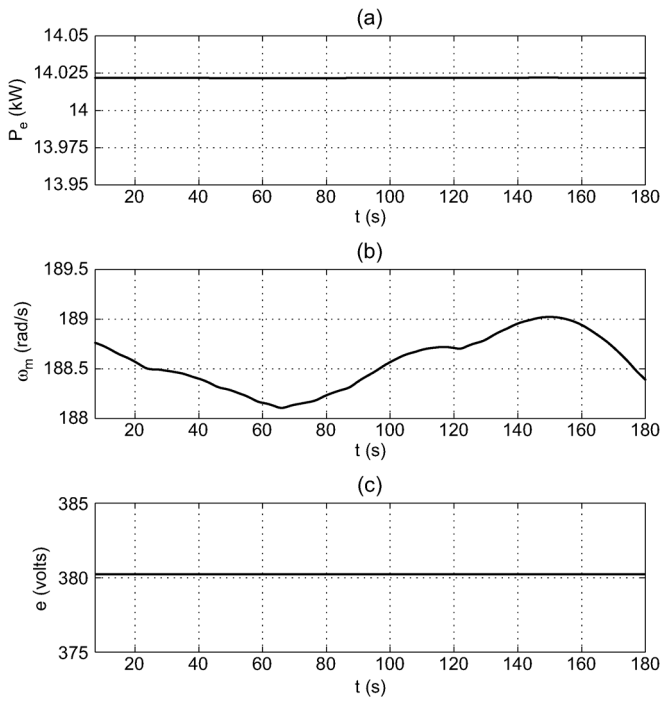

Fig. 9. Simulation results: Generating unit variables for the islanded system.

In the islanded system (Fig. 9), the torque oscillations imposed to the machine are smoothed by the inertia of the rotor and the flywheel. Thus, the average value of the generated power is about 14 kW and the power oscillations are small (0.0014%). Note that, when the instantaneous mechanical power is greater or smaller than the load power, the speed fluctuations reach up to $\pm 0.28\%$ of the rated value [Fig. 9(b)]. The obtained terminal voltage is about 380 V with oscillations of 0.001%.

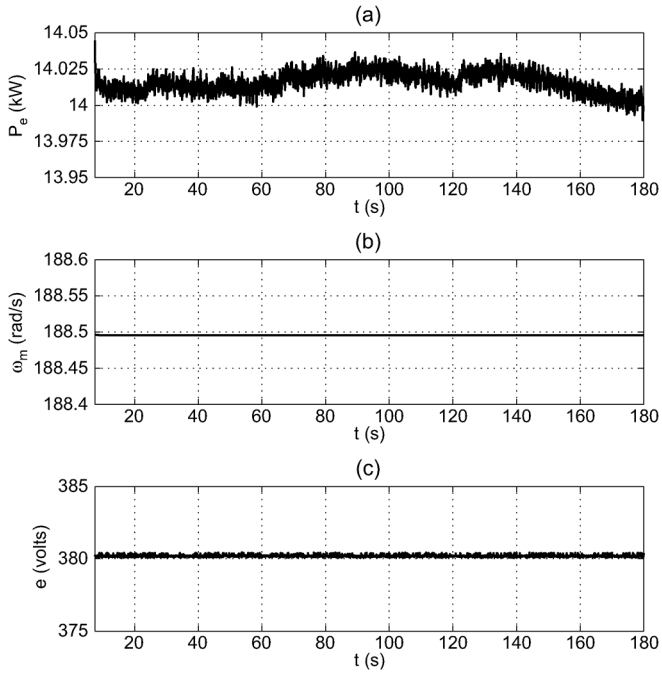

Fig. 10. Simulation results: Generating unit variables for the connected system.

When the generator is connected to the grid (Fig. 10), the initial conditions are chosen such that the generated voltage has the same magnitude, phase angle, and frequency of the grid, to provide synchronism between the generator and the grid. In a real situation, a synchronism relay should be adopted.

From Fig. 10(b), it can be noted that the machine keeps the synchronism with the grid. This is due to the strong characteristic of the simulated grid, which imposes the synchronous speed of the machine. However, it can be inferred that when the system is connected to the grid, as the rotor speed is imposed by the grid, the rotor inertia does not act as a filter, and then, the oscillations observed in the mechanical power [Fig. 8(f)] are transformed directly into electrical power oscillations [Fig. 10(a)]. The average value of the generated power is also 14 kW, and the electric power oscillations are about 0.0022%. The terminal voltage is 380 V.

VII. Conclusion and Future Work

In this study, a complete mathematical wave-to-wire model of the wave energy hyperbaric converter was presented. The main subsystems of the converter were described, and the dynamic models were integrated to evaluate the energy storage of the system. The dynamic model of the accumulator was discussed, and a model for the generating unit was proposed, including a nonlinear model of the hydraulic turbine. Then, the hydrodynamic, mechanical, and electrical characteristics of the main subsystems were discussed and the dynamics of the entire process could be evaluated.

Simulation results considering the proposed dynamic model under the action of regular and irregular incident waves illustrate the performance of the system. The largest value of the chamber volume reduces the amplitude oscillations in the variables, such as pressure, flow, mechanical power, and turbine speed (frequency), as expected, but resulting in higher costs. The power oscillations can be further reduced by including a flywheel in the generating unit. The combination of two storage technologies (gas accumulators and flywheel) allows the size reduction of the hyperbaric chamber, which can reduce the associated costs.

The proposed wave-to-wire model is very useful to address several design and analysis issues without modifying the actual system, for instance, to verify the sensitivity to any system parameter, to implement a fault detection strategy (e.g., to check if the flow rate is within the designed margins), to evaluate the system performance to different wave conditions and the overall efficiency of the WEC, to optimize operating points (e.g., to maximize the absorbed average power), and to optimize the equipment size (e.g., such that acceptable power oscillations can be obtained without oversizing the equipment). The acceptable limits of power oscillation depend on whether the converter is connected to an islanded system, or a weak or strong power grid.

Furthermore, this model can be used in the development and simulation of control strategies to improve the global performance and reliability of the WEC, e.g., frequency/voltage controllers and strategies to improve power absorption and power generation. The integration of control strategies and interlocking mechanisms under different wave climate is an ongoing research work.

References

[1] A. Clément, P. McCullen, A. Falcão, A. Fiorentino, F. Gardner, K. Hammarlund, G. Lemonis, T. Lewis, K. Nielsen, S. Petrocini, M. T. Pontes, P. Schild, B. O. Sjöström, H. C. Sorensen, and T. Thorpe, "Wave energy in Europe: Current status and perspectives," *Renew. Sustain. Energy Rev.*, vol. 6, no. 5, pp. 405–431, 2002.

[2] A. F. O. Falcão, "Wave energy utilization: A review of the technologies," *Renew. Sustain. Energy Rev.*, vol. 14, no. 3, pp. 899–918, 2010.

[3] R. Henderson, "Design, simulation, and testing of a novel hydraulic power take-off system for the pelamis wave energy converter," *Renew. Energy*, vol. 31, no. 2, pp. 271–283, 2006.

[4] A. F. O. Falcão, "Modelling and control of oscillating-body wave energy converters with hydraulic power take-off and gas accumulator," *Ocean Eng.*, vol. 34, pp. 2021–2032, 2007.

[5] C. Josset, A. Babarit, and A. H. Clément, "A wave-to-wire model of the SEAREV wave energy converter," *Proc. Inst. Mech. Eng. M, J. Eng. Maritime Environ.*, vol. 221, no. 2, pp. 81–93, 2007.

[6] I. A. Ivanova, O. Ågren, H. Bernhoff, and M. Leijon, "Simulation of wave-energy converter with octagonal linear generator," *IEEE J. Ocean. Eng.*, vol. 30, no. 3, pp. 619–629, Jul. 2005.

[7] C. Bostrom, R. Waters, E. Lejerskog, O. Svensson, M. Stalberg, E. Stromstedt, and M. Leijon, "Study of a wave energy converter connected to a nonlinear load," *IEEE J. Ocean. Eng.*, vol. 34, no. 2, pp. 123–127, Apr. 2009.

[8] S. Tyrberg, R. Waters, and M. Leijon, "Wave power absorption as a function of water level and wave height: Theory and experiment," *IEEE J. Ocean. Eng.*, vol. 35, no. 3, pp. 558–564, Jul. 2010.

[9] K. Rhinefrank, A. Schacher, J. Prudell, T. K. A. Brekken, C. Stillinger, J. Z. Yen, S. G. Ernst, A. von Jouanne, E. Amon, R. Paasch, A. Brown, and A. Yokochi, "Comparison of direct-drive power takeoff systems for ocean wave energy applications," *IEEE J. Ocean. Eng.*, vol. 37, no. 1, pp. 35–44, Jan. 2012.

[10] J. M. Carrasco, L. G. Franquelo, J. T. Bialasiewicz, E. Galvan, R. C. P. Guisado, M. A. M. Prats, J. I. Leon, and N. Moreno-Alfonso, "Power-electronic systems for the grid integration of renewable energy sources: A survey," *IEEE Trans. Ind. Electron.*, vol. 53, no. 4, pp. 1002–1016, Jun. 2006.

[11] L. Margheritini, D. Vicinanza, and P. Frigaard, "SSG wave energy converter: Design, reliability and hydraulic performance of an innovative overtopping device," *Renew. Energy*, vol. 34, no. 5, pp. 1371–1380, 2009.
[12] J. Cruz, *Ocean Wave Energy: Current Status and Future Prepectives*, ser. Green Energy and Technology. New York, NY, USA: Springer-Verlag, 2008.
[13] Y. Li and Y.-H. Yu, "A synthesis of numerical methods for modeling wave energy converter-point absorbers," *Renew. Sustain. Energy Rev.*, vol. 16, no. 6, pp. 4352–4364, 2012.
[14] P. B. Garcia-Rosa, F. Lizarralde, and S. F. Estefen, "Optimization of the wave energy absorption in oscillating-body systems using extremum seeking approach," in *Proc. Amer. Control Conf.*, Montréal, QC, Canada, 2012, pp. 1011–1016.
[15] J. Falnes, *Ocean Waves and Oscillating Systems: Linear Interaction including Wave-Energy Extraction*. Cambridge, U.K.: Cambridge Univ. Press, 2002.
[16] F. Wu, X.-P. Zhang, P. Ju, and M. J. H. Sterling, "Modeling and control of AWS-based wave energy conversion system integrated into power grid," *IEEE Trans. Power Syst.*, vol. 23, no. 3, pp. 1196–1204, Aug. 2008.
[17] M. Amundarain, M. Alberdi, A. J. Garrido, and I. Garrido, "Modeling and simulation of wave energy generation plants: Output power control," *IEEE Trans. Ind. Electron.*, vol. 58, no. 1, pp. 105–117, Jan. 2011.
[18] K. Ruehl, T. K. A. Brekken, B. Bosma, and R. Paasch, "Large-scale ocean wave energy plant modeling," in *Proc. IEEE Conf. Innovative Technol. Efficient Reliable Electricity Supply*, 2010, pp. 379–386.
[19] S. F. Estefen, P. R. Costa, E. Ricarte, and M. M. Pinheiro, "Wave energy hyperbaric device for electricity production," in *Proc. 26th Int. Conf. Offshore Mech. Arctic Eng.*, San Diego, CA, USA, 2007, pp. 627–633.
[20] S. F. Estefen, P. T. T. Esperança, E. Ricarte, P. R. Costa, M. M. Pinheiro, C. H. P. Clemente, D. Franco, E. Melo, and J. A. Souza, "Experimental and numerical studies of the wave energy hyperbaric device for electricity production," in *Proc. 27th Int. Conf. Offshore Mech. Arctic Eng.*, Estoril, Portugal, 2008, pp. 811–818.
[21] P. B. Garcia-Rosa, J. P. V. S. Cunha, F. Lizarralde, S. F. Estefen, and P. R. Costa, "Efficiency optimization in a wave energy hyperbaric converter," in *Proc. Int. Conf. Clean Electr. Power*, Capri, Italy, 2009, pp. 68–75.
[22] P. R. Costa, P. B. Garcia-Rosa, and S. F. Estefen, "Phase control strategy for a wave energy hyperbaric converter," *Ocean Eng.*, vol. 37, no. 17, pp. 1483–1490, 2010.
[23] P. B. Garcia-Rosa, J. P. V. S. Cunha, and F. Lizarralde, "Turbine speed control for an ocean wave energy conversion system," in *Proc. Amer. Control Conf.*, Saint Louis, MO, USA, 2009, pp. 2749–2754.
[24] E. Ricarte, S. F. Estefen, A. L. T. Mendes, and C. E. Parente, "Wave climate analysis for a wave energy conversion application in Brazil," in *Proc. 26th Int. Conf. Offshore Mech. Arctic Eng.*, San Diego, CA, USA, 2007, pp. 897–902.
[25] W. E. Cummins, "The impulse response function and ship motions," *Schiffstechnik*, vol. 47, no. 9, pp. 101–109, 1962.
[26] E. D. Jaeger, N. Janssens, B. Malfliet, and F. V. D. Meulebroeke, "Hydro turbine model for system dynamic studies," *IEEE Trans. Power Syst.*, vol. 9, no. 4, pp. 1709–1715, Nov. 1994.
[27] P. Kundur, *Power System Control and Stability*, ser. EPRI-Power System Engineering. New York, NY, USA: McGraw-Hill, 1994.
[28] P. C. Krause, O. Wasynczuk, and S. D. Sudhoff, *Analysis of Electric Machinery*. New York, NY, USA: IEEE Press, 1995.
[29] C. H. Lee and J. N. Newman, "WAMIT User Manual Version 6.3, 6.3PC and 6.3S, 6.3S-PC," 1998.
[30] *IEEE Recommended Practice for Excitation System Models for Power System Stability Studies*, IEEE Std 421.5-1992, 1992.
[31] *Rotating Electrical Machines Part 1: Rating and Performance*, IEC 60034-1, 2004.
[32] D. B. Murray, J. G. Hayes, D. L. O. Sullivan, and M. G. Egan, "Supercapacitor testing for power smoothing in a variable speed offshore wave energy converter," *IEEE J. Ocean. Eng.*, vol. 37, no. 2, pp. 301–308, Apr. 2012.
[33] L. Moskowitz, "Estimates of the power spectrums for fully developed seas for wind speeds of 20 to 40 knots," *J. Geophys. Res.*, vol. 69, no. 24, pp. 5161–5179, 1964.
[34] S. Elgar, R. T. Guza, and R. J. Seymour, "Wave group statistics from numerical simulations of a random sea," *Appl. Ocean Res.*, vol. 7, no. 2, pp. 93–96, 1985.

Paula B. Garcia-Rosa (S'13) was born in Rio de Janeiro, Brazil. She received the B.Sc. degree in electronic engineering from the State University of Rio de Janeiro, Rio de Janeiro, Brazil, in 2004, the M.Sc. degree in electrical engineering and the D.Sc. degree in ocean engineering from the COPPE/Federal University of Rio de Janeiro, Rio de Janeiro, Brazil, in 2008 and 2013, respectively.

Her research interests include automation and control of industrial processes, nonlinear control systems, renewable energy technologies and modeling, optimization and control of ocean energy systems.

Ms. Garcia-Rosa is a member of the Sociedade Brasileira de Automática and a student member of the IEEE Control Systems and Oceanic Engineering Societies.

José Paulo Vilela Soares Cunha (S'90–M'92–S'01–M'04) was born in Rio de Janeiro, Brazil, on March 9, 1965. He received the B.Sc. degree in electrical engineering from the State University of Rio de Janeiro, Rio de Janeiro, Brazil, in 1988 and the M.Sc. and D.Sc. degrees in electrical engineering from the Federal University of Rio de Janeiro, Rio de Janeiro, Brazil, in 1992 and 2004, respectively.

From 1992 to 1996, he was a Teacher at the Centro Federal de Educação Tecnológica do Rio de Janeiro, Rio de Janeiro, Brazil. Since 1997, he has been a Professor at the Department of Electronics and Telecommunication Engineering of the State University of Rio de Janeiro. His research interests include sliding-mode control, control of electromechanical systems, robotics, marine systems, underwater and surface vehicles, the development of instrumentation, and measurement systems.

Dr. Cunha is a member of the Sociedade Brasileira de Automática and of the IEEE Control Systems and Oceanic Engineering Societies.

Fernando Lizarralde (S'94–M'01) was born in Bell Ville, Argentina. He received the Ingeniero Electricista degree from the Universidad Nacional del Sur, Bahia Blanca, Argentina, in 1989 and the M.Sc. and Ph.D. degrees in electrical engineering from the Federal University of Rio de Janeiro, Rio de Janeiro, Brazil, in 1992 and 1998, respectively.

He spent 1989 as a Research Fellow at the Universidad Nacional del Sur. In 1994–1995, he was a Visiting Scholar at the Rensselaer Polytechnic Institute, Troy, NY, USA. Since 1996, he has been with the Department of Electrical Engineering, Federal University of Rio de Janeiro, where he is currently an Associate Professor. In 2010–2011, he was a Visiting Researcher at the Center for Automation Technologies and Systems, Rensselaer Polytechnic Institute. His current research interests include nonlinear control systems, adaptive control, variable structure control, visual servoing, stability and oscillations of nonlinear systems and their applications to industrial process control including thermal systems, industrial and cooperative robotics, and underwater robotics.

Prof. Lizarralde is a member of the Sociedade Brasileira de Automática and of the IEEE Control Systems Society. Currently, he is an Associate Editor for the IEEE Control Systems Society Conference Editorial Board.

Segen F. Estefen received the Ph.D. degree in civil engineering from the Imperial College of Science, Technology, and Medicine, London, U.K., in 1984.

He is a Full Professor of Ocean Structures and Subsea Engineering and the Director of Technology and Innovation at the COPPE/Federal University of Rio de Janeiro, Rio de Janeiro, Brazil. He is also the Head of the Subsea Technology Laboratory and Coordinator of the Ocean Renewable Energy Group. He coordinated the Ocean Energy chapter for the Special Report on Renewable Energy of the International Panel of Climate Change. He has more than 150 papers published in journals and conferences.

Prof. Estefen is a member of the Advisory Committee of the Ocean, Offshore and Arctic Engineering Division of the American Society of Mechanical Engineers and the Society for Underwater Technology (SUT) Fellow.

Isaac R. Machado received the B.Sc. and M.Sc. degrees in electrical engineering from the Federal University of Ceará, Ceará, Brazil, in 2004 and 2007, respectively. Currently, he is working toward the Ph.D. degree in electrical engineering at the COPPE/Federal University of Rio de Janeiro, Rio de Janeiro, Brazil.

He is an Assistant Professor at the Federal University of Ceará, Sobral, Ceará, Brazil. He has training in electric power systems, working mainly in the following areas: processing power, drives electrical machinery, industrial automation, and power electronics applied to renewable energy resources.

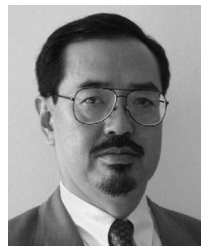

Edson H. Watanabe (S'76–M'77–SM'02) received the B.Sc. degree in electronic engineering and the M.Sc. in electrical engineering from the Federal University of Rio de Janeiro, Rio de Janeiro, Brazil, in 1975 and 1976, respectively, and the D.Eng. degree in electrical engineering from Tokyo Institute of Technology, Tokyo, Japan, in 1981.

In 1981, he joined the COPPE/Federal University of Rio de Janeiro, Rio de Janeiro, Brazil, as an Associate Professor and, since 1994, he has been a Professor. His main field of interest is power electronics applications to power systems, including active power filters, instantaneous active and reactive power theory, HVDC systems, and FACTS.

Prof. Watanabe is a Senior Member of the Power Engineering, Power Electronics, Industry Applications, and Industrial Electronics Societies of the IEEE. He is also a member of the Institute of Electrical Engineers, Japan (IEEJ), the Brazilian Society of Automatic Control, and the Brazilian Society of Power Electronics. In 2005, he was admitted to the National Order of Scientific Merit by a presidential decree (Brazil) and is the recipient of Nari Hingorani 2013 FACTS Award. He is also the coauthor of the book *Instantaneous Power Theory and Applications to Power Conditioning* (New York, NY, USA: IEEE Press/ Wiley, 2007).